RESEARCH ARTICLE | AUGUST 06 2019

Extreme brightness laser-based neutron pulses as a pathway for investigating nucleosynthesis in the laboratory

Special Collection: Special Issue on Extreme High-Field Physics Driven by Lasers

S. N. Chen; F. Negoita; K. Spohr; E. d'Humières; I. Pomerantz; J. Fuchs

Matter Radiat. Extremes 4, 054402 (2019)
https://doi.org/10.1063/1.5081666

Matter and Radiation at Extremes | RESEARCH ARTICLE | scitation.org/journal/mre

Extreme brightness laser-based neutron pulses as a pathway for investigating nucleosynthesis in the laboratory

Cite as: Matter Radiat. Extremes 4, 054402 (2019); doi: 10.1063/1.5081666
Submitted: 15 November 2018 • Accepted: 10 June 2019 •
Published Online: 6 August 2019

S. N. Chen,[1,2] F. Negoita,[1] K. Spohr,[1] E. d'Humières,[3] I. Pomerantz,[4] and J. Fuchs[2,5,a)]

AFFILIATIONS

[1] ELI-NP, "Horia Hulubei" National Institute for Physics and Nuclear Engineering, 30 Reactorului Street, RO-077125 Bucharest-Magurele, Romania
[2] Institute of Applied Physics, 46 Ulyanov Street, 603950 Nizhny Novgorod, Russia
[3] Université Bordeaux, CNRS, CEA, CELIA, UMR 5107, F-33405 Talence, France
[4] School of Physics and Astronomy, Tel-Aviv University, Tel-Aviv 69978, Israel
[5] LULI–CNRS, Ecole Polytechnique, CEA; Université Paris-Saclay; UPMC Université Paris 06; Sorbonne Université, F-91128 Palaiseau cedex, France

[a)] julien.fuchs@poytechnique.fr

ABSTRACT

With the much-anticipated multi-petawatt (PW) laser facilities that are coming online, neutron sources with extreme fluxes could soon be in reach. Such sources would rely on spallation by protons accelerated by the high-intensity lasers. These high neutron fluxes would make possible not only direct measurements of neutron capture and β-decay rates related to the r-process of nucleosynthesis of heavy elements, but also such nuclear measurements in a hot plasma environment, which would be beneficial for s-process investigations in astrophysically relevant conditions. This could, in turn, finally allow possible reconciliation of the observed element abundances in stars and those derived from simulations, which at present show large discrepancies. Here, we review a possible pathway to reach unprecedented neutron fluxes using multi-PW lasers, as well as strategies to perform measurements to investigate the r- and s-processes of nucleosynthesis of heavy elements in cold matter, as well as in a hot plasma environment.

I. INTRODUCTION: STATEMENT OF THE PROBLEM

The overall picture of the production of the hadronic elements around us, starting with primordial hydrogen, is quite clear:[1] fusion of light elements up to and including iron, and various nucleosynthesis processes to form heavier elements. For mid-heavy elements, the dominant process is the so-called s(low)-process (Fig. 1). With this process, heavier elements are generally formed by the absorption of a single neutron on stable isotopes until a radioactive one is reached and this is followed by a β decay before another neutron capture occurs. The s-process takes place in stars over millions of years (Fig. 2) and has been repeatedly tested in the laboratory using accelerators and reactors.[2–4] However, this type of nucleosynthesis ceases to be effective at the quasi-stable element ^{209}Bi,[5] because following a further neutron capture and a β decay, ^{210}Po is subject to α decay, thus reducing the mass number A and limiting further growth of the nucleus. Therefore, to turn these heavy elements into even heavier ones, another process was postulated,[3] namely, the so-called r(apid)-process.

The rapid squeezing of more neutrons into the nucleus of the r-process (Fig. 1)[1] is thought to be the main route to elements beyond Bi, and to roughly half the elements heavier than iron.[3] This process leads to a rapid increase in the mass number A, and it is followed by a β^- decay (emission of an electron and an antineutrino), which in turn leads to an increase in atomic number Z. It is generally accepted that this process can occur only under an extremely high neutron flux [$>10^{20}$ n/(cm^2 s)][6] (see Fig. 2) that is sufficient for multiple neutron captures to take place despite the small cross-sections involved. There is still extensive debate, however, regarding the sites where such a source can exist (e.g., supernova explosions or neutron star mergers)

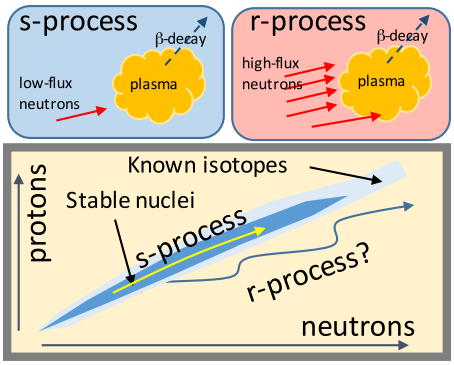

FIG. 1. Illustrations of (bottom) the domain where hadronic elements exist as a function of their proton and neutron numbers and (top) the two main processes of nucleosynthesis. The s(low)-process[2] produces elements along the central domain of known elements. The r(apid)-process proceeds off-center elements through multiple neutron captures.[1]

and regarding the dynamics of the process,[7–12] although we note here that most recent theoretical models have predicted that the r-process elements originate mainly from merging binary neutron stars. The latter prediction has received support from the recent discovery of the first such merger event through the detection of gravitational waves (GW170817)[13] associated with a short γ-ray burst (GRB170817A)[14] and a kilonova (AT2017gfo),[15] whose measured radiation properties are compatible with the model predictions for a radioactively heated ejecta cloud containing high yields of r-process nuclei.

Although the precise threshold at which the r-process takes place is not known, we do know that the required neutron flux is higher than can be produced by any current laboratory neutron source machine (see Fig. 2). To date, on Earth, it has been possible to realize the r-process only in thermonuclear tests,[16,17] with up to 17 successive neutron captures.

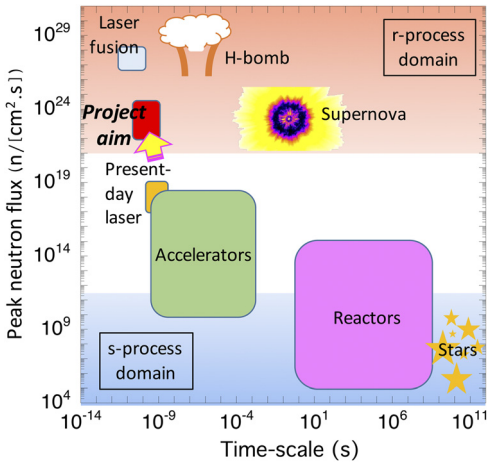

FIG. 2. Peak neutron flux vs time scale of neutron sources produced in various astrophysical sites and in facilities on Earth, showing the parameters at which the s(low)- and r(apid)-processes of nucleosynthesis take place.

At present, it is possible to measure only some of the basic nuclear properties related to the r-process, such as the masses and decay rates of superheavy elements, by creating neutron-rich isotopes through fission and spallation in existing facilities.[12] The possibility of using ever heavier nuclei for doing this has motivated in part the construction of a new generation of large-scale, high-energy radioactive ion facilities, such as the Radioactive Isotope Beam Factory (RIBF) at RIKEN, the upcoming Facility for Rare Isotope Beams (FRIB) at Michigan State University, and Facility for Antiproton and Ion Research (FAIR) in Darmstadt.[2,10] However, because these radioactive ion facilities are separate from neutron sources, neutron capture rates cannot be measured on radioactive/unstable elements even for single neutrons. Furthermore, multiple neutron capture rates cannot be measured even on relatively stable elements, because the neutron flux produced by existing machines is too low, as illustrated in Fig. 2 and detailed in Table I. It should also be noted that the neutron energies of interest in astrophysics are only those between 1 keV and a few hundreds of keV, and hence facilities producing thermal neutrons [e.g., integrated injection logic (IIL)], or spallation moderated sources [e.g., Spallation Neutron Source (SNS)] are not particularly useful. Only continuous quasi-stellar beams (e.g., LiLiT, FRANZ, and HISPANOS) or time-of-flight facilities (e.g., nTOF, DANCE, and GELINA) are of use.

Furthermore, at these upcoming radioactive ion facilities,[18,19] with the exception of the NIF laser fusion facility,[20] we must rely on theory and simulations for analysis of measurements, and the large uncertainties regarding nuclear data[20–22] on the involved heavy nuclei prevent us from gaining knowledge about the dynamics of the r-process. Our understanding of the r-process is at present limited by these uncertainties, as well as by the difficulties inherent in astrophysical modeling.[23]

A further difficulty with measurements performed using accelerators and reactors, whether aimed at the s- or the r-process, is that they are carried out in "cold" conditions, i.e., not in a plasma environment that can strongly affect the properties of the nuclei.[24–27] This is usually referred to as the stellar enhancement factor (SEF).[28] Electron or photon interactions with a nucleus in a plasma environment can excite the nucleus to higher energy states, including nuclear isomers. Excitation and decay rates of nuclei in plasmas can vary, compared with entropies present in the solid state, by many orders of magnitude, even at thermal temperatures of a few hundreds of eV.[29–31] Such excited states of the nucleus and its changed internal energy structure[18,26,32] will directly affect the neutron absorption cross-section (notably for $A > 150$)[33] compared with that of the ground state. Electron screening[34] is another effect that is theoretically believed to affect nuclear reaction rates and β-decay rates in a plasma environment, especially at low projectile energies, which are those most relevant both in astrophysics and for Inertial Confinement Fusion (ICF). In nuclear reactions, to an incoming charged particle, a fully or partially ionized atom "looks" less negatively charged; in a decaying isotope, the presence of an unoccupied electron shell increases the chance of emission of an electron from the nucleus, compared with the case of a neutral atom.[35–37] This is mostly the case for low nuclear energy levels, below approximately 100 keV. The neutron capture rate is further influenced by the changed excitation energy, spin, and parity of the compound state and angular momentum barriers in particle transitions.[20,24]

The r-process is further complicated by the involvement of fission recycling such that under an intense neutron flux, the neutron-

TABLE I. Comparative overview of neutron beam characteristics produced at existing facilities generating the most intense neutron beams and those that will be produced by upcoming multi-PW lasers (in bold).

Facility	Peak neutron flux [n/(cm^2 s)]	Average neutron flux [n/(cm^2 s)]	Neutron bunch duration	Repetition rate (Hz)
ILL (reactor-based)[39]	$\sim 10^{15}$	$\sim 10^{15}$	(Continuous)	(Continuous)
SNS (accelerator-based)[39]	$\sim 10^{16}$	$\sim 10^{12}$	~ 1 μs	60
Present-day lasers[46,47,49]	10^{18}–10^{19}	5×10^5–5×10^6	~ 1 ns	5×10^{-4} (1 shot/30 min)
Upcoming multi-PW lasers	$\mathbf{10^{22}}$–$\mathbf{5 \times 10^{24}}$	$\mathbf{10^{11}}$–$\mathbf{5 \times 10^{13}}$	**~ 1 ns**	$\mathbf{1.6 \times 10^{-2}}$ **(1 shot/min)**
NIF (laser-fusion-based)[20]	$>10^{26}$	$>10^{10}$	~ 10 ps	10^{-5} (1 shot/day)

induced fission products of heavy elements produced by neutron capture(s) can themselves be subject to neutron capture(s). The fission product distribution has a decisive effect on final abundances, but the theoretical nuclear models of such processes have significant uncertainties.[38] A related issue is that the outcome of the r-process, namely, the final element abundances, depends not only on the reaction rates, but also on the initial seed abundance, i.e., which heavy elements are present in the plasma that is subject to the r-process, and in what fractions.[1,10,18] This could explain why there seem to be two patterns of element abundances produced by the r-process,[7,10] although this explanation has not been yet tested.

Compared with the existing facilities described above, new players are emerging, namely ultra-high-power (multi-petawatt, PW) lasers, which could provide a sharp increase in the neutron fluxes available. In turn, this would allow direct measurements of the r-process, as well as the s-process, in heavy elements. Furthermore, these measurements could also become feasible in a plasma environment, allowing investigation of the above-mentioned impact of such environments compared with cold matter. It is the aim of the present paper to describe these new developments.

II. SHORT-PULSE LASER-ACCELERATED NEUTRONS: A NEW TOOL

Over the last decade, high-power lasers have opened the door to many important discoveries related to astrophysical phenomena (in the field of so-called "laboratory astrophysics"[40–43]). With PW-class lasers,[44] as discussed below, it will be possible to generate, through spallation driven by laser-accelerated protons, the short duration and high neutron flux needed for investigations of the s-process[45] and r-process. Note that laser-based production of high-flux neutrons has already been demonstrated by several groups,[46–50] using lasers in the several hundred terawatt (TW) class.

This type of neutron production rests on the generation, by high-power lasers, of bunches of ions of extreme brightness (mega-amperes and picoseconds at the source, in a single shot).[51] In the absence of special surface treatment of the target irradiated by the laser, protons stemming from surface contaminants (mainly water) are the most prevalent. These ions can then be converted into neutrons using a variety of nuclear reactions in low-atomic-weight isotopes, the most common being D(d, n) and Li(p, n). Alternatively, (γ, n) reactions, where γ rays are induced by high-energy electrons, can be exploited in high-Z materials, leading also to efficient neutron generation.[47] At existing laser facilities, this has been shown to lead to neutrons of extremely short pulse duration (<50 ps) and high peak flux of $>10^{18}$ n/(cm^2 s). Table I shows a comparison between the best neutron beams produced by reactors, accelerators, and lasers. Note that with respect to peak brightness, laser-based beams are already competitive, but because of the low repetition rate (at best 1 shot per 20 min) of the present high-energy, high-power lasers, the average brightness is quite low compared with that of other types of sources.

Below, we discuss the possibility offered by the upcoming PW and multi-PW class lasers to significantly increase the neutron flux and the repetition rate, bringing these to the levels required for r-process investigations. Note that there are many such facilities, either already open, for example at the University of Texas (USA),[52] SIOM (China),[53] and GITS (Korea),[54] or under construction, ranging from 10 PW class lasers, such as those at Apollon (France)[55] and the ELI facilities (Czech Republic[56] and Romania[57]), to 100 PW ones, such as SEL (China).[58] Because these upcoming laser facilities are equipped with auxiliary high-energy laser pulses, the possibility exists of simultaneously generating the type of hot plasmas that emulate astrophysical conditions, which is a unique feature of this class of accelerators. The added advantage here is that it is possible to perform a "pump–probe" experiment in which one laser can create a plasma, which will evolve on a nanosecond time scale, and another can "probe" (in this case, to create a neutron beam) on a picosecond/femtosecond time scale. By sending the neutron beam faster than the evolution of the plasma target, what the neutron beam "sees" is essentially frozen in time.

Although these auxiliary lasers cannot create every plasma state that exists in the universe, a large range of conditions can be created, namely, densities ranging from gaseous to solid and temperatures ranging from room temperature to thousands of eV. Sites for the r-process include supernova explosions or neutron star mergers, both with extreme densities ($\gg$solid density) and temperatures ($>10^4$ eV), and there are currently no methods by which these exact conditions can be achieved in the laboratory. Laser-created plasmas do, however, offer one of the only ways in which it might be possible to create such high-energy-density plasmas (HEDPs) in the laboratory, and indeed they have already been used to study a variety of astrophysical phenomena.[40–43]

Figure 3 illustrates the concept of an experimental platform that would take advantage of upcoming multi-PW lasers to allow s- and r-process investigations in plasmas. In more detail, the arrangement shown in Fig. 4 is composed of three main blocks: (a) the generation and transport of a high-density, high-energy proton beam (blocks 1 and 2), (b) the production of neutrons (block 3), and (c) the nucleosynthesis experiments proper (blocks 4 and 5). These are discussed in detail below. Note that stages (a) and (b), with the notable

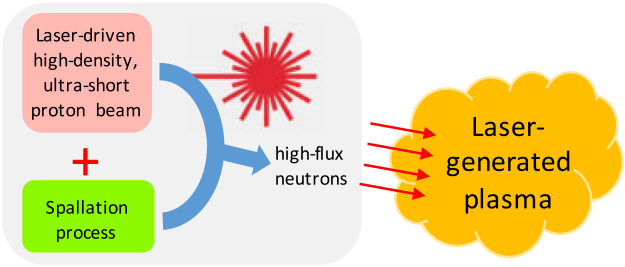

FIG. 3. Cartoon of a setup that would allow, with a multi-PW laser as a driver, the investigation of r-process nucleosynthesis in the laboratory.

capability of high throughput and short final duration (nanoseconds) of the produced neutrons, have already been demonstrated,[49] albeit at lower neutron fluxes than envisioned with upcoming multi-PW lasers.

A. Producing a high-energy, high-density, ultra-short proton source

The first step necessary to reach efficient neutron production, through spallation, with lasers is to improve the energy of laser-accelerated protons. To this end, the energy of the protons needs to be increased because the spallation conversion efficiency is strongly dependent on the incident proton energy.[59] With present-day lasers, limited to on-target intensities below 10^{21} W/cm^2 (Fig. 5), the maximum proton energy is just below 100 MeV,[60–62] with around 10^{13} protons in the bunch (and 100% energy spread, the spectrum being close to Maxwellian[51]). Therefore, to date, with the neutrons being produced using the aforementioned nuclear reactions, from ~10^8 (Ref. 63) to ~3×10^9 (Ref. 46) neutrons can be produced in a single shot, which means that the efficiency is at best ~10^{-2}.

The upcoming multi-PW lasers should make it possible to push the focused intensity of the laser beam on target by at least one order of magnitude (Fig. 5) to 10^{22} W/cm^2, and even further to 10^{23} W/cm^2 with the help of refocusing plasma optics to reduce the laser focal spot and boost the focused intensity.[64,65] As shown in Fig. 5, the immediate consequence should be an increase in the maximum energy of the produced protons. Most notably, the domain of maximum energy above 200 MeV should be reached, making it possible to significantly increase the throughput of neutron production by spallation, as will be discussed below. A notable second advantage of the upcoming multi-PW lasers is that because of a change in the laser pumping

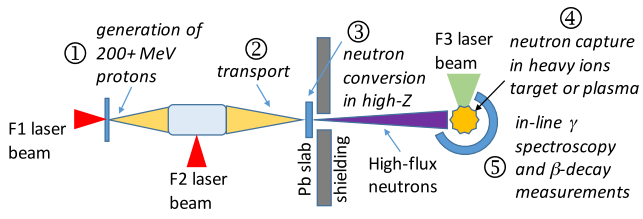

FIG. 4. Possible multi-PW laser-based platform to allow s- and r-process investigations in plasmas. The circled numbers correspond to different stages of the platform (see text).

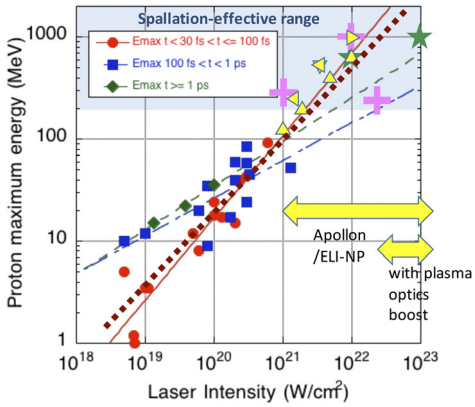

FIG. 5. Scaling of the maximum proton energy as a function of the laser intensity on target, with trendlines. Circles, squares, and diamonds are experimental points, showing that the 100 MeV threshold has been reached at today's intensities. Crosses and stars represent simulations performed by our group using various targets (the crosses stand for RPA and the stars for SA). The yellow triangles correspond to the simulation results of Refs. 69–72, and the brown dashed line is the theoretical scaling from Ref. 73.

schemes, these facilities will produce laser pulses at much higher repetition rates than present-day facilities, from 1 shot/min to 1 Hz. This will result in a strong increase in the average neutron brightness that these facilities will generate (see Table I).

The expected increase in proton energy following from the increased laser intensity is not the result of brute force, but of a transition to different acceleration mechanisms that promise to be inherently more efficient. With the laser intensities accessible today, the most efficient ion acceleration mechanism is of an electrostatic type that develops at the surface of the laser-irradiated solid target, powered by a dense and hot Debye sheath of electrons, accelerated by the laser pulse and residing in vacuum, i.e., so-called target normal sheath acceleration (TNSA).[51] Most of the next-generation multi-PW facilities will have beams carrying hundreds of joules in energy. The conversion efficiency using the TNSA mechanism is about 1%, which means the accelerated ion beam will carry several joules of energy and likely ~10^{11} protons having hundreds of MeV energy.

With the intensities that will be accessible with multi-PW lasers, an improvement on these numbers could be expected through promising new acceleration mechanisms[51] that should become available, namely radiation pressure acceleration (RPA) and shock acceleration (SA). The RPA mechanism relies on ultra-thin (nanometer) targets[51] and very clean laser pulses, which should also be characteristic of the upcoming laser facilities, while SA relies on tailored target density profiles.[66,67] Both mechanisms provide better scaling with laser intensity as well as lower-divergence beams than TNSA, but the laser-to-proton conversion efficiency, nominally of a few percent[51] and at best 15%,[68] should also improve significantly. Our 2D particle-in-cell (PIC) simulations, using the parameters of upcoming laser facilities such as Apollon, show the possibility of reaching maximum energies higher than 200 MeV in both the mixed TNSA/RPA and SA regimes (see the crosses and stars in Fig. 5), with ~10^{13} protons/shot over the whole broadband distribution and ~10^{12} protons/shot in the high-energy range of hundreds of MeV.

B. Proton beam transport to the neutron converter

After generating the high-density, high-energy proton beams, it is necessary to transport them away from the violent radiation streams (X rays, γ rays, and electrons) induced by the laser–target interaction (step 2 in Fig. 4). It is also necessary to focus the proton beam to obtain the highest neutron flux possible (per unit surface).[49,74] To do so, conventional accelerator optics can be used,[75] but these are limited in their beam acceptance, proton number, and spectrum, thereby limiting the overall transported charge. Rather, a compact (millimeter-scale), plasma-based and laser-triggered micro-lens can be used.[76] This consists of a hollow cylinder (from inexpensive millimeter-diameter tubing or 3D-printed) that is irradiated by a pulse from an auxiliary short-pulse laser (Fig. 4). The auxiliary laser launches a high number (~10^{14}) of MeV-energy electrons normal to the inner walls of the cylinder, which induce radially symmetric transient electric fields inside. Such fields act to focus protons transiting along the axis of the cylinder. As we have demonstrated, the focusing is extremely repeatable, ensuring stable conditions for the final transported proton beam. Because the fields produced in the device are of the order of gigavolts per meter, an extremely compact setup is possible, reducing travel time and temporal stretching of the proton beam inside the focusing device, which should provide refocusing over a ~0.1 mm spot at 0.5 m distance. As shown in Fig. 6, simulations[77] and models[78] have already shown that this optic is adapted to transporting and focusing protons having an energy >200 MeV. Only a 10^{20} W/cm^2 intensity laser beam is needed to drive this focusing plasma lens.

C. Efficient production of high-brightness neutrons

Once the proton beam has been transported and refocused away from the laser-driven ion source, we need efficient conversion into neutrons (step 3 in Fig. 4). As noted above, resorting to spallation promises great improvement over existing work with lasers. Spallation is a process that occurs when a light projectile (a proton, neutron, or light ion) with a kinetic energy from several hundreds of MeV to several GeV interacts with a heavy nucleus (e.g., lead) and causes the emission of a large number of hadrons (mostly neutrons).[59,79] Figure 7 illustrates a neutron spectrum resulting from the spallation of a 1 GeV energy input proton beam in a 2 cm thick Pb target, obtained with the FLUKA code.[80,81] We have tested different configurations for spallation, namely, a broadband input proton beam with a Maxwellian or a flat-top distribution, and observed little variation in the output neutron beam. Using a reduced-energy (250 MeV maximum energy) proton beam, we expect a similar output neutron beam to be produced, although with a reduced conversion efficiency (around 1 neutron/proton).

Overall, with the protons that we expect to produce at multi-PW facilities like Apollon or ELI-NP, we should generate >10^{12} neutrons in the output of the Pb converter. Using a conservative estimate of 50% for the proton beam bandwidth, it will debunch over ~0.7 ns after 50 cm, i.e., by the time it reaches the Pb spallation converter. Taking this as the duration of the neutron bunch (as the individual spallation process takes place over a ~10^{-22} s time scale), and a source size imposed by the protons scattering in the Pb target (radius over 3 mm for protons at 250 MeV and 0.5 mm at 1 GeV), the conservatively estimated resulting peak flux will be ~10^{22}–5×10^{23} n/(cm^2 s) (Fig. 2). Note that with a reduced (10%) bandwidth proton beam, the neutron bunch could be reduced to ~50 ps, and the flux further increased by one order of magnitude, i.e., up to 5×10^{24} n/(cm^2 s).

As noted above, because the repetition rate of the multi-PW lasers will be improved compared with present-day lasers, the time-averaged neutron flux should also become quite high. Using a repetition rate of 1 shot/min (for the largest facilities), the time-averaged neutron flux should reach ~10^{11}–5×10^{12} n/(cm^2 s), which will greatly exceed those available on existing facilities (see Table I) and should permit multiple neutron capture.[21,82] As an alternative to spallation, it should also be possible to exploit (γ, n) reactions in a high-Z nucleus, as has already been tested in present-day facilities,[47]

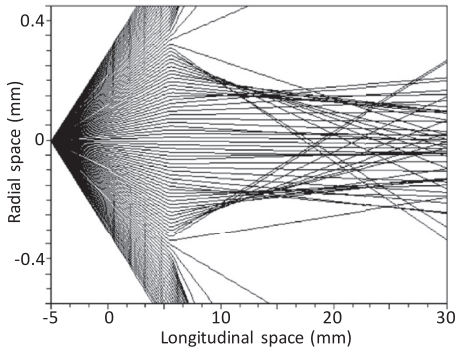

FIG. 6. PIC simulations of a wide-angle divergent (~20° full-angle) proton beam emitted from a point source on the left and being focused as it propagates to the right. The focusing element is a cylinder of length 6 mm (its entrance being at position 0 in the figure) and diameter 700 μm that is irradiated on its side by a laser pulse having 10^{20} W/cm^2 intensity. Note that, for clarity, the two axes are not scaled similarly. The trajectories of 100 protons at 270 MeV are plotted, showing that the protons are well focused and collimated over long distances after the micro-lens.

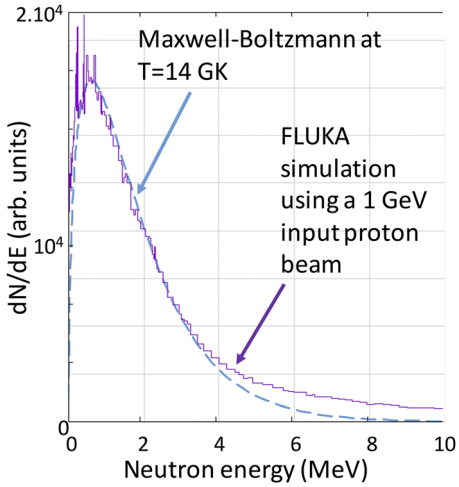

FIG. 7. Simulated neutron spectrum obtained by spallation in a 2 cm thick Pb target of a laser-driven proton beam, using the FLUKA particle transport Monte Carlo code.[81] The spallation yield is 10 neutrons/proton. The dashed line represents the thermal spectrum, indicating that the spectral shape is not far from the conditions expected for the r-process.

which could produce a peak neutron flux of 10^{20} $n/(\mathrm{cm}^2\ \mathrm{s})$. Furthermore, the neutron spectrum shown in Fig. 7 will be close to a ~14 GK thermal spectrum (dashed blue line), with a peak around 600 keV, i.e., conditions that are somewhat high but not far from those postulated for r-process realization in supernovas.[1]

Such a high-flux neutron bunch can be characterized by standard neutron detection techniques that have commonly been used by the laser-plasma community[49,83–88] and include shielded CR39 track detectors, bubble detectors, activation in samples positioned after the neutron beam, and neutron time-of-flight (nTOF) measurements. It should also be possible to use alternative emerging techniques, offering, for example, improved immunity to laser-induced noise and improved sensitivity.[89–91]

III. PEAK FLUX REQUIREMENTS FOR MULTI-NEUTRON CAPTURE MEASUREMENTS

We now turn to a numerical evaluation of multi-neutron capture reaction yields resulting from high peak-flux neutron irradiation. The derivation we follow is described in detail in Ref. 92. The rate equation for single-neutron capture of a (Z, A) isotope is

$$\frac{dN_{Z,A}}{dt} = N_{Z,A-1} n_0 \sigma^{Z,A-1} - N_{Z,A} n_0 \sigma^{Z,A} - N_{Z,A} \lambda_{Z,A},$$

where n_0 is the peak neutron flux, $\sigma^{Z,A}$ is the neutron capture cross-section, and $\lambda_{Z,A}$ is its prominent decay rate. Solving this equation gives the relative yield of the $(Z, A + k)$ isotope:

$$N_{Z,A+k} = \frac{x^k}{k!} e^{-x} \prod_i^k e^{-\tau_n \lambda_{Z,A+i}},$$

where $\tau_n = (n_0 \sigma^{Z,A})^{-1}$ is the neutron capture time, and $x = n_0 \tau \sigma^{Z,A}$ is the average number of captured neutrons. τ_n is the key parameter that determines the reaction yields: for the r-process to prevail, τ_n must be smaller than each of the half-lives of the isotopes in the production chain.

We evaluate the neutron capture yields on a sample of ^{96}Zr for various experimental scenarios. ^{96}Zr is a stable isotope with a natural abundance of 2.8%. The half-lives of the Zr isotopes considered here are listed in Table II.

In general, capture cross-sections for *fast* neutrons have a smooth dependence on their energy. For the purpose of this analysis, a constant value of $\sigma^{Z,A} = 1$ b is assumed for all isotopes. Actual cross-section values can be integrated easily into these results.

Figure 8 presents the results of our evaluation. A present-day, laser-based neutron generator outputs a 1 ns long pulse with a peak flux of 10^{18} $n/(\mathrm{cm}^2\ \mathrm{s})$. The corresponding neutron capture time is $\tau_n = 10^6$ s, which is close to the ^{97}Zr half-life (produced by a single-neutron capture). In this case, τ_n is much longer than the half-lives of heavier Zr isotopes, and therefore only single-neutron captures occur. The produced ^{97}Zr isotopes will eventually decay by β emission. This, in essence, is the s-process.

TABLE II. Half-lives of $^{96-102}$Zr isotopes.

^{96}Zr	^{97}Zr	^{98}Zr	^{99}Zr	^{100}Zr	^{101}Zr	^{102}Zr
Stable	17 h	31 s	2.1 s	7.1 s	2.3 s	2.9 s

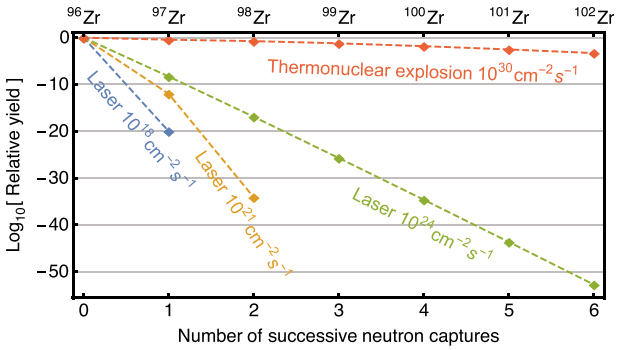

FIG. 8. Relative yields of isotopes produced by successive multi-neutron captures, i.e., by the r-process. The seed target is ^{96}Zr. The peak neutron flux is indicated for each curve. Laser experiments are calculated for a pulse duration of 1 ns. Also shown are the relative yields produced by a 1 μs long thermonuclear explosion.

The peak flux of 10^{24} $n/(\mathrm{cm}^2\ \mathrm{s})$ expected in the upcoming multi-PW lasers corresponds to a neutron capture time of $\tau_n = 1$ s. This capture time is shorter than all the $^{97-102}$Zr isotope half-lives, and multi-neutron capture yields can be calculated (green curve in Fig. 8). For comparison, Fig. 8 also presents the multi-neutron capture yields that will result from a single 1 μs long thermonuclear explosion.

IV. STRATEGY FOR NUCLEOSYNTHESIS EXPERIMENTS

Single-neutron capture in stable elements at room-temperature conditions is very well established and measured with high accuracy at accelerator- and reactor-based facilities. The unique opportunities that multi-PW laser facilities would now open are to perform neutron capture in (1) plasmas and (2) unstable nuclei. These two types of measurements can be performed using two different setups, illustrated in Figs. 9 and 10, respectively.

A. Neutron capture in a plasma

Setup (1) would indeed allow measurement of single-neutron capture in hot plasma conditions for the first time. However, β-decay

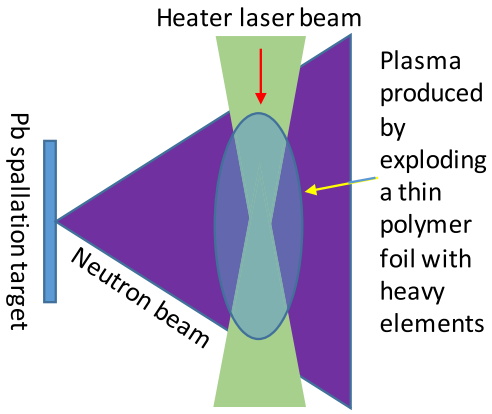

FIG. 9. Proposed setup for neutron capture measurements in hot plasmas.

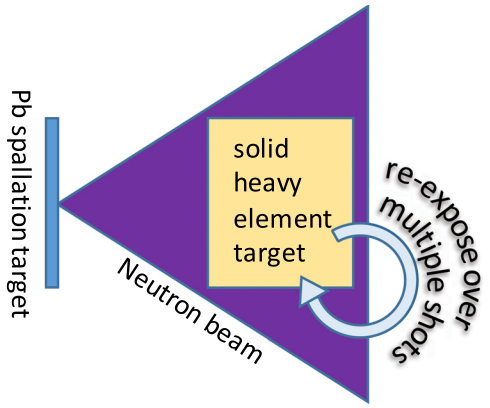

FIG. 10. Proposed setup for double-neutron capture measurements.

measurement cannot be performed, because the created plasma will have disassembled before the β-decay can take place. There are several ways of producing these hot and dense plasmas. A well-assessed technique, illustrated in Fig. 9, is to explode a thin (~1 μm) film with a long-pulse auxiliary laser beam.[93] Such a film can be made of a light element, polymer-based, and doped with heavy elements. Using such a film, it is easy to produce a plasma with a density of 10^{20} cm^{-3} at temperatures up to 1 keV, i.e., in a regime relevant to investigating plasma effects.[29,31] For example, in a plasma exploded over a ~0.3 mm diameter and ~1 mm length, and having a 1% admixture of heavy elements, ~10^{14} ions will be exposed, over a 1 ns duration, to ~10^{13} n/cm^2. Using a typical neutron absorption cross-section of 100 mb,[82,94] ~10^2 isotopes will be produced. Such a setup would further allow (i) testing of final abundances when the density of the doped element is varied and (ii) measurements of neutron-induced fission cross-sections.[22,38] A plastic or metal foam[95] could serve as an alternative target material. Its advantage would be that the plasma produced (over the same millimeter scale length) is denser (densities 10^{21}–10^{22} cm^{-3} can be easily achieved) and more homogeneous than what can be achieved by exploding thin foils, but it is also colder ~10–100 eV. In this case, the target consists of a polyimide tube filled with an ultra-low-density plastic foam doped by a heavy element that is heated by X rays, produced by a long-pulse laser irradiating a Cu foil placed at one end of the tube.

B. Experiments with unstable nuclei

Setup (2), illustrated in Fig. 10, would allow the first measurements of both the neutron capture rate and β decay in unstable nuclei. It would use a thick target exposed to the intense neutron flux. It would then be possible to generate unstable nuclei in the exposed target, and re-expose it on the next shot to the neutrons, to perform a second neutron capture. For example, the calculation shows that using a 10 cm thick ^{238}U target exposed over 1 cm^2 to the neutrons, and again with a typical neutron absorption cross-section of about 100 mb, ~5×10^{11} ^{239}U isotopes will be produced in the first stage (with a half-life of 23.45 min), resulting in 0.5 ^{240}U isotopes (with a 14.1 h half-life) through double-neutron capture in the second stage. This number is certainly not high, but it is within the accepted range of achievable measurements.[82] With 1 shot/min, which will be achievable with the upcoming multi-PW facilities, it will be possible to measure on average 50 events per day. This compares favorably with the planned month-long exposure for similar double-neutron capture measurements using upcoming high-flux accelerator-based facilities[45] The experiment could be performed on elements located in the peak in abundances near atomic mass 130, because their capture and decay properties affect the abundances of heavier elements.[1,94] For example, the elements $^{130-132}$Sb and $^{129-131}$Sn have half-lives between a few minutes and a few tens of minutes and therefore could be appropriate for measurements using the proposed platform. Note further that at ELI-NP, there will be a production line of unstable nuclei through photo-fission induced by a record-brilliance γ beam (this is a stand-alone capability, independent of the two 10 PW laser beams that will be available at this facility), followed by slowing down in noble gas and subsequent extraction.[96]

C. Measurement

The diagnostics used in both of these configurations would rely mostly on γ spectrometry. Following a neutron capture by an element having atomic mass and number (A, Z), the produced unstable nucleus having ($A+1$, Z) is in an excited state. It relaxes to the ground state over a fast time scale (pico- to nanoseconds) by emitting γ rays. By measuring these promptly emitted γ rays, we can measure the amount of produced unstable nuclei, N_{products}. Also, once in its ground state, the unstable nucleus can β-decay. This takes place over longer time scales, the fastest decays taking place over milliseconds. The product of the decay will also be in an excited state, and it will also emit γ rays. By measuring these, we will be able to determine the number of decaying states, i.e., the desired N_{products}. Thus, there will be two successive stages of γ emission. The first will produce a much larger amount of γ radiation than the second, but since there is a significant time lag between the two stages, we will be able to differentiate the two emissions. Note that such β-decay measurement makes sense only for the experiment related to double-neutron capture (Fig. 10). For neutron capture in a plasma (Fig. 9), it will not be useful, because the plasma will disassemble before the β decay takes place. Therefore, the β decay would be characteristic only of ground-state nuclei, and this is already measured using existing facilities.[97] Note also that the separation between the laser-interaction and neutron-capture locations (Fig. 4) will be important to avoid pile-up in the γ-ray detector due to the laser-generated γ rays. As discussed above, it would also be necessary to characterize the incident neutron beam, i.e., determine F_n, the neutron flux (per unit surface). Finally, with knowledge of the number of atoms in the target, $N_{\text{reactants}}$, the desired cross-section for neutron capture, σ, can be inferred[98] as $\sigma = N_{\text{products}}/(N_{\text{reactants}} \times F_n)$. Note that this is a direct procedure, distinct from the recently developed indirect methods that use so-called "surrogate reactions" in which existing radioactive nuclei are made to interact with light-nuclei targets to arrive at the same states as those produced by neutron capture.[99] By measuring reaction products with γ radiation and then using models, it is possible to derive the neutron capture rate, so that measurements can be performed on elements far from the valley of stability.[100] This represents a significant advance, but it remains highly model-dependent.

For both (1) and (2), the emitted γ rays can be measured using existing instrumentation, i.e., through arrays of detectors, combining scintillators and photomultipliers. In our proposed setup (Fig. 4), the

large separation between the high-intensity laser interaction, with its associated high-radiation environment, and the neutron–matter interaction point will be important to allow reduced background measurements. Note that when performing measurements using a plasma target, the γ rays we expect to be emitted will be easily distinguishable from the plasma background, their energies being much higher than those of the soft X rays emitted by the plasma, which can be blocked. Each short-lived nuclear element has its specific energy and lifetime, which makes it possible to identify it unambiguously through the γ rays it will emit, even if several elements are present simultaneously within the target.

V. CONCLUSION AND PERSPECTIVES

We have here outlined a strategy that would open a pathway, using upcoming multi-PW laser facilities, for laboratory investigations of the s- and r-processes, including direct measurements of double-neutron capture events and measurements in hot plasmas in order to go toward astrophysically relevant measurements. We expect with the next generation of multi-PW lasers to improve our understanding of all processes related to nucleosynthesis by helping nuclear physics models achieve better anchors for the capture cross-sections they use.[12] We note that the upcoming multi-PW laser facilities such as Apollon in France and the ELIs in Eastern Europe will start their commissioning in 2019–2020, opening to users in the following year. We expect that pushing the performances of ion and neutron beams will be a significant part of the research performed on these facilities, in particular at Extreme Light Infrastructure Nuclear Physics (ELI-NP), with its emphasis on nuclear physics. Hence, a first assessment of the possibility of obtaining measurements relevant to r-process nucleosynthesis should be obtainable within the next five years.

We have shown that the extreme brightness of the neutrons allowed by the presented setup will allow measurements of r-process cross-section, but we should note that the platform outlined here can also be used for advancing our understanding of s-process reactions within a hot and dense plasma environment, for which there is again little knowledge based on measurements.

Aside from nucleosynthesis, we also expect extreme-brightness neutron sources, such as the one proposed here, based on upcoming laser facilities, to have a broad collateral effect. The compact and high-brightness beamline we envision creating could help satisfy the increasing demand for neutron sources,[101] such as those intended for radioisotope production and even for more futuristic transmutation applications. This demand will be difficult to meet with conventional facilities because of their associated cost. As in these conventional facilities, the neutrons produced by lasers are fast (from hundreds of keV to MeV; see Fig. 7), but this is not a limiting factor, because it has recently been shown[50] that laser-based pulsed neutrons can be moderated without losing the benefit of sub-nanosecond duration. Furthermore, a neutron source with the aforementioned characteristics will be a significant improvement over other current (fast) neutron sources, and will open new paths for applications for the larger physics community. Fast-neutron probing and imaging[86,102–104] is a powerful tool with both civilian and military applications,[105–107] including radiation hardness testing of semiconductors for spacecraft, materials for fusion or fission reactors, and particle accelerator vessels or containers for storing radioactive nuclear waste, to name only a few. Increasing the neutron flux, as proposed here, would greatly increase the sensitivity of detection for all these applications.

ACKNOWLEDGMENTS

We acknowledge fruitful discussions with H. Pépin (INRS), V. Méot, L. Gremillet, X. Davoine (CEA), S. Orlando (INAF), C. Guerrero (Universidad de Sevilla), and Y. Caristan (Université Paris-Saclay). This project received funding from the European Research Council (ERC) under the European Union's Horizon 2020 Research and Innovation Programme (Grant Agreement No. 787539), and was partly conducted within the LABEX Plas@Par project and supported by Grant Nos. 11-IDEX-0004-02 and an ANR-17-CE30-0026 PiNNaCLE grant from Agence Nationale de la Recherche (France). I.P. acknowledges the support of ISF Grant No. 1135/15. The research leading to these results is supported by Extreme Light Infrastructure Nuclear Physics (ELI-NP) Phase I, a project co-financed by the Romanian Government and the European Union through the European Regional Development Fund.

REFERENCES

[1]M. Arnould *et al.*, "The r-process of stellar nucleosynthesis: Astrophysics and nuclear physics achievements and mysteries," Phys. Rep. **450**, 97 (2007).
[2]C. Lederer *et al.*, "Experiments with neutron beams for the astrophysical s process," J. Phys.: Conf. Ser. **665**, 012020 (2016).
[3]E. M. Burbidge *et al.*, "Synthesis of the elements in stars," Rev. Mod. Phys. **29**, 547 (1957).
[4]R. Reifarth *et al.*, "Neutron reactions in astrophysics," J. Phys. G: Nucl. Part. Phys. **41**, 053101 (2014).
[5]U. Ratzel *et al.*, "Nucleosynthesis at the termination point of the s-process," Phys. Rev. C **70**, 065803 (2004).
[6]J. J. Cowan *et al.*, "R-process nucleosynthesis in dynamic helium-burning environments," Astrophys. J. **294**, 656 (1985).
[7]F.-K. Thielemann *et al.*, "What are the astrophysical sites for the r-process and the production of heavy elements?," Progr. Part. Nucl. Phys. **66**, 346–353 (2011).
[8]N. R. Tanvir *et al.*, "A 'kilonova' associated with the short-duration γ-ray burst GRB 130603B," Nature **500**, 547 (2013).
[9]W. R. Binns *et al.*, "Observation of the ^{60}Fe nucleosynthesis-clock isotope in galactic cosmic rays," Science **352**, 677 (2016).
[10]A. P. Ji *et al.*, "R-process enrichment from a single event in an ancient dwarf galaxy," Nature **531**, 610 (2016).
[11]G. M. Fuller *et al.*, "Primordial black holes and r-process nucleosynthesis," Phys. Rev. Lett. **119**, 061101 (2017).
[12]C. J. Horowitz *et al.*, "r-process nucleosynthesis: Connecting rare-isotope beam facilities with the cosmos," J. Phys. G: Nucl. Part. Phys. **46**, 83001 (2019).
[13]B. P. Abbott *et al.*, "GW170817: Observation of gravitational waves from a binary neutron star in spiral," Phys. Rev. Lett. **119**, 161101 (2017).
[14]E. Pian *et al.*, "Spectroscopic identification of r-process nucleosynthesis in a double neutron-star merger," Nature **551**, 67 (2017).
[15]D. Kasen, B. Metzger, J. Barnes, E. Quataert, and E. Ramirez-Ruiz, "Origin of the heavy elements in binary neutron-star mergers from a gravitational-wave event," Nature **551**, 80 (2017).
[16]H. Diamond *et al.*, "Heavy isotope abundances in Mike thermonuclear device," Phys. Rev. **119**, 2000 (1960).
[17]Y. Lutostansky, and V. I. Lyashuk, Transuranium elements production in pulse neutron fluxes, *Proceedings of the 4th International Conference on Current Problems in Nuclear Physics and Atomic Energy, NPAE 2012, Kyiv, Ukraine* (The National Academy of Sciences of Ukraine, 2012), pp. 164–168.
[18]M. R. Mumpower *et al.*, "The impact of individual nuclear properties on r-process nucleosynthesis," Prog. Part. Nucl. Phys. **86**, 86 (2016).

[19]G. Feinberg *et al.*, "LiLiT-a liquid-lithium target as an intense neutron source for nuclear astrophysics at the soreq applied research accelerator facility," Nucl. Phys. A **827**, 590c (2009).
[20]O. A. Hurricane *et al.*, "Fuel gain exceeding unity in an inertially confined fusion implosion," Nature **506**, 343 (2014).
[21]R. Reifarth and Y. A. Litvinov, "Measurements of neutron-induced reactions in inverse kinematics," Phys. Rev. Spec. Top. - Accel. Beams **17**, 014701 (2014).
[22]I. V. Panov, "Nucleosynthesis of heavy elements in the r-process," Phys. At. Nucl. **79**, 159–198 (2016).
[23]H.-T. Janka *et al.*, "Physics of core-collapse supernovae in three dimensions: A sneak preview," Annu. Rev. Nucl. Part. Sci. **66**, 341–375 (2016).
[24]T. Rauscher, "Revision of the derivation of stellar rates from experiment and impact on Eu s-process contributions," J. Phys.: Conf. Ser. **665**, 012024 (2016).
[25]N. Nishimura *et al.*, "Impact of new β-decay half-lives on r-process nucleosynthesis," Phys. Rev. C **85**, 048801 (2012).
[26]G. Gosselin *et al.*, "Nuclear excitation processes in astrophysical plasmas," in *Astrophysics*, edited by I. Kucuk (InTech, London, 2012).
[27]J. N. Ávila *et al.*, "Europium s-process signature at close-to-solar metallicity in stardust SiC grains from asymptotic giant branch stars," Astrophys. J. Lett. **768**, L18 (2013).
[28]T. Rauscher, "Formalism for inclusion of measured reaction cross sections in stellar rates including uncertainties and its application to neutron capture in the s-process," Astrophys. J. Lett. **755**, L10 (2012).
[29]G. Gosselin *et al.*, "Enhanced nuclear level decay in hot dense plasmas," Phys. Rev. C **70**, 064603 (2004).
[30]A. V. Andreev *et al.*, "Excitation and decay of low-lying nuclear states in a dense plasma produced by a subpicosecond laser pulse," J. Exp. Theor. Phys. **91**, 1163 (2000).
[31]G. Gosselin *et al.*, "Modified nuclear level lifetime in hot dense plasmas," Phys. Rev. C **76**, 044611 (2007).
[32]S. Goriely, "Nuclear reaction data relevant to nuclear astrophysics," J. Nucl. Sci. Tech. **39**(suppl. 2), 536 (2002).
[33]T. Rauscher *et al.*, "Opportunities to constrain astrophysical reaction rates for the s-process via determination of the ground-state cross-sections," Astrophys. J. **738**, 143 (2011).
[34]F. Raiola *et al.*, "First hint on a change of the ^{210}Po alpha-decay half-life in the metal Cu," Eur. Phys. J. A **32**, 51 (2007).
[35]K. Takahashi and K. Yokoi, "Beta-decay rates of highly ionized heavy atoms in stellar interiors," At. Data Nucl. Data Tables **36**, 375 (1987).
[36]F. Bosch *et al.*, "Observation of bound-state β-decay of fully ionized ^{187}Re: ^{187}Re^{187}Os cosmochronometry," Phys. Rev. Lett. **77**, 5190 (1996).
[37]Yu. A. Litvinov and F. Bosch, "Beta decay of highly charged ions," Rep. Prog. Phys. **74**, 016301 (2011).
[38]S. Goriely *et al.*, "New fission fragment distributions and r-process origin of the rare-earth elements," Phys. Rev. Lett. **111**, 242502 (2013).
[39]M. N. H. Comsan, http://www.iaea.org/inis/collection/NCLCollectionStore/_Public/43/099/43099436.pdf.
[40]B. A. Remington *et al.*, "Modeling astrophysical phenomena in the laboratory with intense lasers," Science **284**, 1488 (1999).
[41]B. Albertazzi *et al.*, "Laboratory formation of a scaled protostellar jet by coaligned poloidal magnetic field," Science **346**, 325 (2014).
[42]G. Revet *et al.*, "Laboratory unraveling of matter accretion in young stars," Sci. Adv. **3**, e1700982 (2017).
[43]G. Gregori *et al.*, "Generation of scaled protogalactic seed magnetic fields in laser-produced shock waves," Nature **481**, 480–483 (2012).
[44]C. Danson *et al.*, "Petawatt class lasers worldwide," High Power Laser Sci. Eng. **3**, e3 (2015).
[45]C. Guerrero *et al.*, "Prospects for direct neutron capture measurements on s-process branching point isotopes," Eur. Phys. J. A **53**, 87 (2017).
[46]M. Roth *et al.*, "Bright laser-driven neutron source based on the relativistic transparency of solids," Phys. Rev. Lett. **110**, 044802 (2013).
[47]I. Pomerantz *et al.*, "Ultrashort pulsed neutron source," Phys. Rev. Lett. **113**, 184801 (2014).
[48]Y. Arikawa *et al.*, "High-intensity neutron generation via laser-driven photonuclear reaction," Plasma Fusion Res. **10**, 2404003 (2015).
[49]D. P. Higginson *et al.*, "Temporal narrowing of neutrons produced by high-intensity short-pulse lasers," Phys. Rev. Lett. **115**, 054802 (2015).
[50]S. Mirfayzi *et al.*, "Experimental demonstration of a compact epithermal neutron source based on a high power laser," Appl. Phys. Lett. **111**, 044101 (2017).
[51]A. Macchi *et al.*, "Ion acceleration by superintense laser-plasma interaction," Rev. Mod. Phys. **85**, 751 (2013).
[52]E. Gaul *et al.*, "Demonstration of a 1.1 petawatt laser based on a hybrid optical parametric chirped pulse amplification/mixed Nd:glass amplifier," Appl. Opt. **49**, 1676–1681 (2010).
[53]Z. Gan *et al.*, "200 J high efficiency Ti:sapphire chirped pulse amplifier pumped by temporal dual-pulse," Opt. Express **25**, 5169 (2017).
[54]J. H. Sung *et al.*, "4.2 PW, 20 fs Ti:sapphire laser at 0.1 Hz," Opt. Lett. **42**, 2058 (2017).
[55]J. P. Zou *et al.*, "Design and current progress of the Apollon 10 PW project," High Power Laser Sci. Eng. **3**, e2 (2015).
[56]B. Rus *et al.*, "ELI-beamlines: Development of next generation short-pulse laser systems," Proc. SPIE **9515**, 95150F (2015).
[57]R. Dabu, "High power femtosecond lasers at ELI-NP," AIP Conf. Proc. **1645**, 219 (2015).
[58]E. Cartlidge, "The light fantastic," Science **359**(6374), 382–385 (2018).
[59]D. Hilscher, U. Jahnke, F. Goldenbaum, L. Pienkowski, J. Galin, and B. Lott, "Neutron production by hadron-induced spallation reactions in thin and thick Pb and U targets from 1 to 5 GeV," Nucl. Instrum. Methods Phys. Res., Sect. A **414**, 100–116 (1998).
[60]F. Wagner *et al.*, "Maximum proton energy above 85 MeV from the relativistic interaction of laser pulses with micrometer thick CH_2 targets," Phys. Rev. Lett. **116**, 205002 (2016).
[61]I. J. Kim *et al.*, "Radiation pressure acceleration of protons to 93 MeV with circularly polarized petawatt laser pulses," Phys. Plasmas **23**, 070701 (2016).
[62]A. Higginson, "Near-100 MeV protons via a laser-driven transparency-enhanced hybrid acceleration scheme," Nat. Commun. **9**, 724 (2018).
[63]D. P. Higginson *et al.*, "Characterization of a laser-generated neutron source" (unpublished).
[64]M. Nakatsutsumi *et al.*, "Fast focusing of short-pulse lasers by innovative plasma optics toward extreme intensity," Opt. Lett. **35**, 2314–2316 (2010).
[65]M. Nakatsutsumi *et al.*, "Self-generated surface magnetic fields inhibit laser-driven sheath acceleration of high-energy protons," Nat. Commun. **9**, 280 (2018).
[66]F. Fiuza *et al.*, "Laser-driven shock acceleration of monoenergetic ion beams," Phys. Rev. Lett. **109**, 215001 (2012).
[67]S. N. Chen *et al.*, "Collimated protons accelerated from an overdense gas jet irradiated by a 1 μm wavelength high-intensity short-pulse laser," Sci. Rep. **7**, 13505 (2017).
[68]C. M. Brenner *et al.*, "High energy conversion efficiency in laser-proton acceleration by controlling laser-energy deposition onto thin foil targets," Appl. Phys. Lett. **104**, 081123 (2014).
[69]A. A. Sahai *et al.*, "Relativistically induced transparency acceleration of light ions by an ultrashort laser pulse interacting with a heavy-ion-plasma density gradient," Phys. Rev. E **88**, 043105 (2013).
[70]H. Y. Wang *et al.*, "High-energy monoenergetic proton beams from two stage acceleration with a slow laser pulse," Phys. Rev. Spec. Top. - Accel. Beams **18**, 021302 (2015).
[71]A. V. Brantov *et al.*, "Synchronized ion acceleration by ultraintense slow light," Phys. Rev. Lett. **116**, 085004 (2016).
[72]M. L. Zhou *et al.*, "Proton acceleration by single-cycle laser pulses offers a novel monoenergetic and stable operating regime," Phys. Plasmas **23**, 043112 (2016).
[73]A. V. Brantov *et al.*, "Ion energy scaling under optimum conditions of laser plasma acceleration from solid density targets," Phys. Rev. Spec. Top. - Accel. Beams **18**, 021301 (2015).
[74]C. Ellison and J. Fuchs, "Optimizing laser-accelerated ion beams for a collimated neutron source," Phys. Plasmas **17**, 113105 (2010).

[75]S. Busold *et al.*, "Commissioning of a compact laser-based proton beam line for high intensity bunches around 10 MeV," Phys. Rev. Spec. Top. - Accel. Beams **17**, 031302 (2014).
[76]T. Toncian, M. Borghesi, J. Fuchs *et al.*, "Ultrafast laser-driven microlens to focus and energy-select mega-electron volt protons," Science **312**, 410 (2006).
[77]E. d'Humières, J. Fuchs *et al.*, "Proton acceleration: New developments in energy increase, focusing and energy selection," AIP Conf. Proc. **877**, 41 (2006).
[78]S. Gordienko, T. Baeva, and A. Pukhov, "Focusing of laser-generated ion beams by a plasma cylinder: Similarity theory and the thick lens formula," Phys. Plasmas **13**, 063103 (2006).
[79]K. van der Meer *et al.*, "Spallation yields of neutrons produced in thick lead/bismuth targets by protons at incident energies of 420 and 590 MeV," Nucl. Instrum. Methods Phys. Res., Sect. B **217**, 202–220 (2004).
[80]A. Ferrari *et al.*, Fluka: A multi-particle transport code, CERN-2005-10 (2005), INFN/TC_05/11, SLAC-R-773, https://cds.cern.ch/record/898301/files/CERN-2005-010.pdf.
[81]T. T. Böhlen *et al.*, "The FLUKA code: Developments and challenges for high energy and medical applications," Nucl. Data Sheets **120**, 211–214 (2014).
[82]A. Couture and R. Reifarth, "Direct measurements of neutron capture on radioactive isotopes," At. Data Nucl. Data Tables **93**, 807 (2007).
[83]S. Mirfayzi *et al.*, "Calibration of time of flight detectors using laser-driven neutron source," Rev. Sci. Instrum. **86**, 073308 (2015).
[84]A. Alejo *et al.*, "High flux, beamed neutron sources employing deuteron-rich ion beams from D_2O-ice layered targets," Plasma Phys. Controlled Fusion **59**, 064004 (2017).
[85]P. A. Norreys *et al.*, "Neutron production from picosecond laser irradiation of deuterated targets at intensities of 10^{19} W cm^{-2}," Plasma Phys. Controlled Fusion **40**, 175 (1998).
[86]R. K. Fisher *et al.*, "High-resolution neutron imaging of laser fusion targets using bubble detectors," Phys. Plasmas **9**, 2182–2185 (2002).
[87]M. Storm *et al.*, "Fast neutron production from lithium converters and laser driven protons," Phys. Plasmas **20**, 053106 (2013).
[88]C. Zulick *et al.*, "Energetic neutron beams generated from femtosecond laser plasma interactions," Appl. Phys. Lett. **102**, 124101 (2013).
[89]J. M. Gómez-Ros *et al.*, "CYSP: A new cylindrical directional neutron spectrometer. Conceptual design," Radiat. Meas. **82**, 47–51 (2015).
[90]D. Maire *et al.*, "Development of a μ-TPC detector as a standard instrument for low-energy neutron field characterisation," Radiat. Prot. Dosim. **161**, 245–248 (2014).
[91]G. Croci, F. Murtas, and F. Resnati, "Prospects in MPGDs development for neutron detection," arXiv:1601.01534 [physics.ins-det].
[92]V. I. Zagrebaev, A. V. Karpov, I. N. Mishustin, and W. Greiner, "Production of heavy and superheavy neutron-rich nuclei in neutron capture processes," Phys. Rev. C **84**, 044617 (2011).
[93]M. D. Rosen *et al.*, "Exploding-foil technique for achieving a soft X-ray laser," Phys. Rev. Lett. **54**, 106 (1985).
[94]K. H. Guber *et al.*, "Neutron cross section measurements at the spallation neutron source," J. Nucl. Sci. Tech. **39**, 638–641 (2002).
[95]S. N. Chen *et al.*, "Density and temperature characterization of long-scale length, near-critical density controlled plasma produced from ultra-low density plastic foam," Sci. Rep. **6**, 21495 (2016).
[96]S. Gales *et al.*, "New frontiers in nuclear physics with high-power lasers and brilliant monochromatic gamma beams," Phys. Scr. **91**, 093004 (2016).
[97]J. Pereira *et al.*, "β-decay half-lives and β-delayed neutron emission probabilities of nuclei in the region $A \lesssim 100$ relevant for the r process," Phys. Rev. C **79**, 035806 (2009).
[98]A. Paulsen, *Utility and Use of Neutron Capture Cross Section Standards and the Status of the Au(n,y) Standard* (National Bureau of Standards Special Publication, 1977), Vol. 493, p. 165.
[99]J. Escher *et al.*, "Compound-nuclear reaction cross sections from surrogate measurements," Rev. Mod. Phys. **84**, 353–397 (2012).
[100]S. N. Liddick *et al.*, "Experimental neutron capture rate constraint far from stability," Phys. Rev. Lett. **116**, 242502 (2016).
[101]R. Hamm, "Review of industrial accelerators and their applications," in *IAEA Proceedings Series*, Paper AP/IA-12, STI/PUB/1433 (IAEA, 2010), ISBN: 978-92-0-150410-4.
[102]V. Dangendorf *et al.*, "Detectors for energy-resolved fast-neutron imaging," Nucl. Instrum. Methods Phys. Res. Sect. A **535**, 93 (2004).
[103]D. C. Swift *et al.*, "Explanation of anomalous shock temperatures in shock-loaded Mo samples measured using neutron resonance spectroscopy," Phys. Rev. B **77**, 092102 (2008).
[104]N. Guler *et al.*, "Neutron imaging with the short-pulse laser driven neutron source at the Trident laser facility," J. Appl. Phys. **120**, 154901 (2016).
[105]L. J. Perkins *et al.*, "The investigation of high intensity laser driven micro neutron sources for fusion materials research at high fluence," Nucl. Fusion **40**, 1 (2000).
[106]J. D. Sethian *et al.*, "An overview of the development of the first wall and other principal components of a laser fusion power plant," J. Nucl. Mater. **347**, 161 (2005).
[107]U. Fischer *et al.*, "Evaluation and validation of d–Li cross section data for the IFMIF neutron source term simulation," J. Nucl. Mater. **367-370**, 1531 (2007).